Evolution of the vomer and its implications for cranial kinesis in Paraves

Han Hu[a,1], Gabriele Sansalone[a], Stephen Wroe[a], Paul G. McDonald[a], Jingmai K. O'Connor[b,c], Zhiheng Li[b,c], Xing Xu[b,c], and Zhonghe Zhou[b,c,1]

[a]Zoology Division, School of Environmental and Rural Sciences, University of New England, Armidale, NSW 2351, Australia; [b]Key Laboratory of Vertebrate Evolution and Human Origins, Institute of Vertebrate Paleontology and Paleoanthropology, Chinese Academy of Sciences, 10010 Beijing, China; and [c]Chinese Academy of Sciences Center for Excellence in Life and Paleoenvironment, 10010 Beijing, China

Contributed by Zhonghe Zhou, August 6, 2019 (sent for review May 14, 2019; reviewed by Daniel J. Field and Oliver W. M. Rauhut)

Most living birds exhibit cranial kinesis—movement between the rostrum and braincase—in which force is transferred through the palatal and jugal bars. The palate alone distinguishes the Paleognathae from the Neognathae, with cranial kinesis more developed in neognaths. Most previous palatal studies were based on 2D data and rarely incorporated data from stem birds despite great interest in their kinetic abilities. Here we reconstruct the vomer of the Early Cretaceous stem bird *Sapeornis* and the troodontid *Sinovenator*, taxa spanning the dinosaur–bird transition. A 3D shape analysis including these paravians and an extensive sampling of neornithines reveals their strong similarity to paleognaths and indicates that morphological differences in the vomer between paleognaths and neognaths are intimately related to their different kinetic abilities. These results suggest the skull of Mesozoic paravians lacked the kinetic abilities observed in neognaths, a conclusion also supported by our identification of an ectopterygoid in *Sapeornis* here. We conclude that cranial kinesis evolved relatively late, likely an innovation of the Neognathae, and is linked to the transformation of the vomer. This transformation increased palatal mobility, enabling the evolution of a diversity of kinetic mechanisms and ultimately contributing to the extraordinary evolutionary success of this clade.

cranial kinesis | palate | stem birds | Neornithes | Jehol

Neornithes is the only surviving lineage of the Dinosauria and with more than 10,000 living species represents the most diverse clade of extant amniotes (1, 2). The survival of Neornithes through the End-Cretaceous mass extinction has been attributed to numerous key biological adaptations (3–6), but their current diversity has also been attributed to the specialized architecture of their skulls (7, 8). Cranial kinesis, movement of the skull, in particular movement of the rostrum independent of the braincase, is present in most living birds, occurring in a variety of forms strongly associated with specialized feeding mechanisms (9–11). Cranial kinesis is made possible through the complete reduction of the postorbital bar and loss of the ectopterygoid, and the occurrence of the flexible area in the rostrum and the mobile quadrate and the palatal complex (consisting of the palatine, vomer, and pterygoid), which transfers force from the quadrate to elevate the upper bill at the various intracranial joints and zones of flexion (12–15). Mobility and flexibility of the palate are extremely important elements of cranial kinesis. Notably, differences in palatal morphology are also generally accepted as the best known characters capable of diagnosing the deepest dichotomy in the Neornithes: the Paleognathae and the Neognathae (16–18). The Neognathae account for the vast majority of the current avian diversity and are characterized by much more extensive cranial kinesis compared to paleognathous species (2, 13, 14, 19).

Cranial kinesis has been the subject of great interest since first described. However, nearly all previous work on the avian palate has been based on traditional qualitative observations of 2D views of the more easily observed palatine and pterygoid (7, 11–15, 17, 20). Such studies fail to capture the true 3D morphology of this complex structure. Furthermore, the vomer has been largely overlooked as vestigial and difficult to reveal a significant pattern in the Neognathae (11, 17, 21). Although this element is reduced in the Neognathae and even lost in several clades, the variation of this element between different orders, as revealed by this study, still indicates its important functional role in the palatal complex.

The closest nonavian dinosaurian relatives of Aves are thought to have akinetic skulls with an unreduced palatal complex (7, 22). Although the fossil record of stem birds and their closest relatives has grown enormously over the past 3 decades (23), detailed information concerning palatal morphology in these taxa is extremely rare due to their delicate nature and the crushed, 2D preservation of most specimens. With only few exceptions, the palate is partially preserved in 2D in some specimens of the Late Jurassic *Archaeopteryx* (24–26), the Early Cretaceous enantiornithine *Chiappeavis* (27), the Late Cretaceous enantiornithine *Gobipteryx* (28, 29), the Late Cretaceous ornithurine *Ichthyornis* (30), and ambiguously in *Hesperornis* (31, 32). Consequently, despite great interest, the origin of the modern avian palate and cranial kinesis from the akinetic nonavian theropod condition remains poorly understood (8, 30, 32, 33).

Here we provide 3D data of the vomer from an Early Cretaceous bird—the early-diverging pygostylian *Sapeornis chaoyangensis* (34), together with information from the troodontid *Sinovenator*, a

Significance

Cranial kinesis is an important feature of neornithine birds. However, due to the rarity of palatal elements in fossils, its origin is poorly understood. Here we reconstruct the vomer of the troodontid *Sinovenator* and the stem bird *Sapeornis*, and provide the palatal reconstruction of this Early Cretaceous bird. Using these data we conducted a comprehensive morphological study of the palate and a 3D shape analysis of the vomer across Paraves. The results indicate that stem birds, like palaeognaths, had limited cranial kinesis, a conclusion also supported by the identification of an ectopterygoid in *Sapeornis*. This suggests that the remarkably flexible avian skull is a neognathous innovation, with greater cranial kinesis ultimately facilitating the radiation of this highly successful lineage.

Author contributions: H.H., G.S., S.W., P.G.M., J.K.O., Z.L., X.X., and Z.Z. designed research; H.H., G.S., S.W., P.G.M., J.K.O., Z.L., X.X., and Z.Z. performed research; H.H. and G.S. analyzed data; and H.H., G.S., and J.K.O. wrote the paper.

Reviewers: D.J.F., University of Cambridge; and O.W.M.R., Bayerische Staatssammlung für Paläontologie und Geologie.

The authors declare no conflict of interest.

Data deposition: 3D models, landmarks and semilandmarks, and phylogenetic tree are available at Figshare (DOI: 10.6084/m9.figshare.7769279.v2).

[1]To whom correspondence may be addressed. Email: huhan@ivpp.ac.cn or zhouzhonghe@ivpp.ac.cn.

This article contains supporting information online at www.pnas.org/lookup/suppl/doi:10.1073/pnas.1907754116/-/DCSupplemental.

First published September 9, 2019.

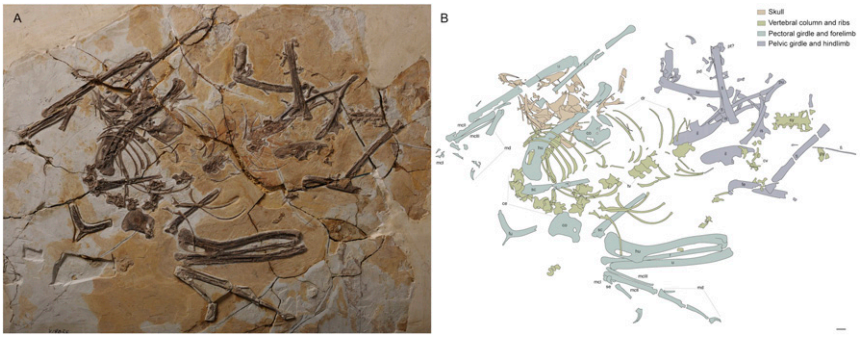

Fig. 1. Full-slab photograph (*A*) and camera lucida drawing (*B*) of *S. chaoyangensis*, IVPP V19058. Abbreviations: ce, cervical vertebrae; co, coracoid; cv, caudal vertebrae; dr, dorsal ribs; fe, femur; fi, fibula; fr, frontal; fu, furcula; hu, humerus; il, ilium; is, ischium; mc, metacarpal; md, manual digit; pd, pedal digits; pt, proximal tarsals; pu, pubis; py, pygostyle; r, radius; sc, scapula; se, semilunate carpal; sy, synsacrum; ti, tibia; tv, thoracic vertebrae; u, ulna; and v, vomer. (Scale bar: 1 cm.)

nonavian dinosaur phylogenetically positioned close to the dinosaur–bird transition (35, 36). Morphological information is provided for the palate of *Sapeornis*, enabling a preliminary reconstruction of the palate for this Early Cretaceous bird. Based on these data and the 3D models of the vomer in these 2 extinct taxa and representatives of extant neornithines, we conduct a comprehensive morphological study of the avian palate and a 3D geometric morphometric analysis focusing on the vomer, in order to infer the evolutionary trends in the palate across Paraves and explore the cranial kinetic abilities of stem birds and the origin of the highly kinetic avian skull.

Results

Morphological Descriptions. The specimen of *S. chaoyangensis* Institute of Vertebrate Paleontology and Paleoanthropology (IVPP) V19058 was collected from the Lower Cretaceous Yixian Formation at the Sihedang locality near Lingyuan in Liaoning province. It is inferred to represent a late-stage subadult, such that palatal morphology would not be expected to be significantly affected by further development (Fig. 1 and *SI Appendix*, Table S1; for detailed taxonomic and ontogenetic information see *SI Appendix*, *Supplementary Methods*). The disarticulated cranial elements include a complete vomer, left ectopterygoid, and an element tentatively identified as the right palatine (Fig. 2 *A* and *B*).

The cranial portion of the vomer is fused with the caudal portion diverging into 2 caudolaterally oriented flanges; the lateral margins are weakly convex (Fig. 3*A*). A similar morphology has also been described in some nonavian dinosaurs, e.g., *Gobivenator* (37), the most primitive bird *Archaeopteryx* (24–26), and some modern birds, especially within the Paleognathae. Although the vomer is very poorly represented in stem birds, our survey of previously published specimens of *Sapeornis* identified morphologically similar structures preserved nearly in situ in 2 other articulated specimens: preserved between the left and right premaxillae and maxillae in Shandong Tianyu Museum of Nature, China (STM) 16–18 (Fig. 3*B*) and slightly dislocated between the rostrum and mandibles in IVPP V13275 (Fig. 3*C*; originally described as the splenial, but clearly distinct from the in situ and complete splenial preserved in *Sapeornis* STM 16–18)

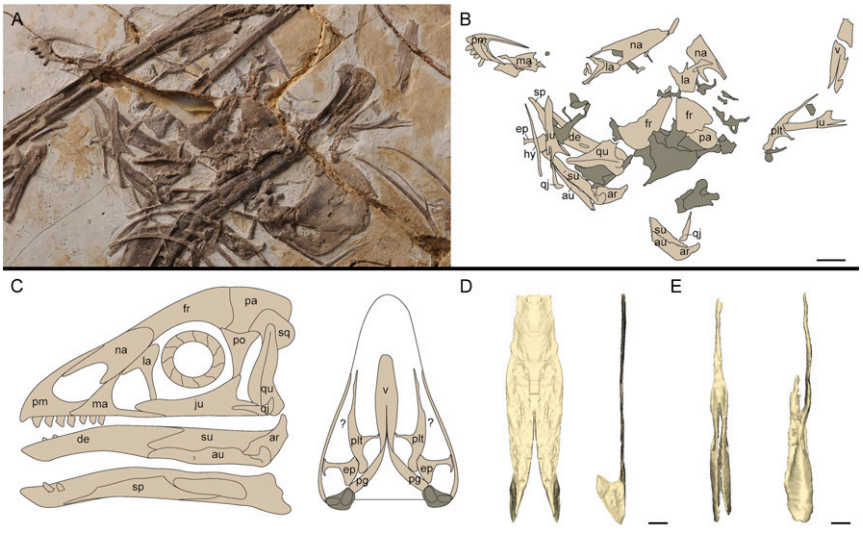

Fig. 2. (*A*) Detailed photograph and (*B*) camera lucida drawing of the skull of *Sapeornis* IVPP V19058. (*C*) Cranial reconstructions of *Sapeornis* (lateral cranium, lateral mandible, labial mandible, and ventral cranium). (*D*) Three-dimensional reconstructed and retrodeformed vomer of *Sapeornis* IVPP V19058 in ventral and lateral view. (*E*) Three-dimensional reconstructed vomer of *Sinovenator* IVPP V12615 in ventral and lateral view. Dark gray indicates uncertain elements, and question marks indicate the uncertain jugal processes of palatines. Abbreviations: au, angular; ar, articular; de, dentary; ep, ectopterygoid; fr, frontal; hy, hyoid; ju, jugal; la, lacrimal; ma, maxilla; na, nasal; pa, parietal; pm, premaxilla; pg, pterygoid; plt, palatine; po, postorbital; qj, quadratojugal; qu, quadrate; sp, splenial; sq, squamosal; su, surangular; and v, vomer. (Scale bar: 1 cm.)

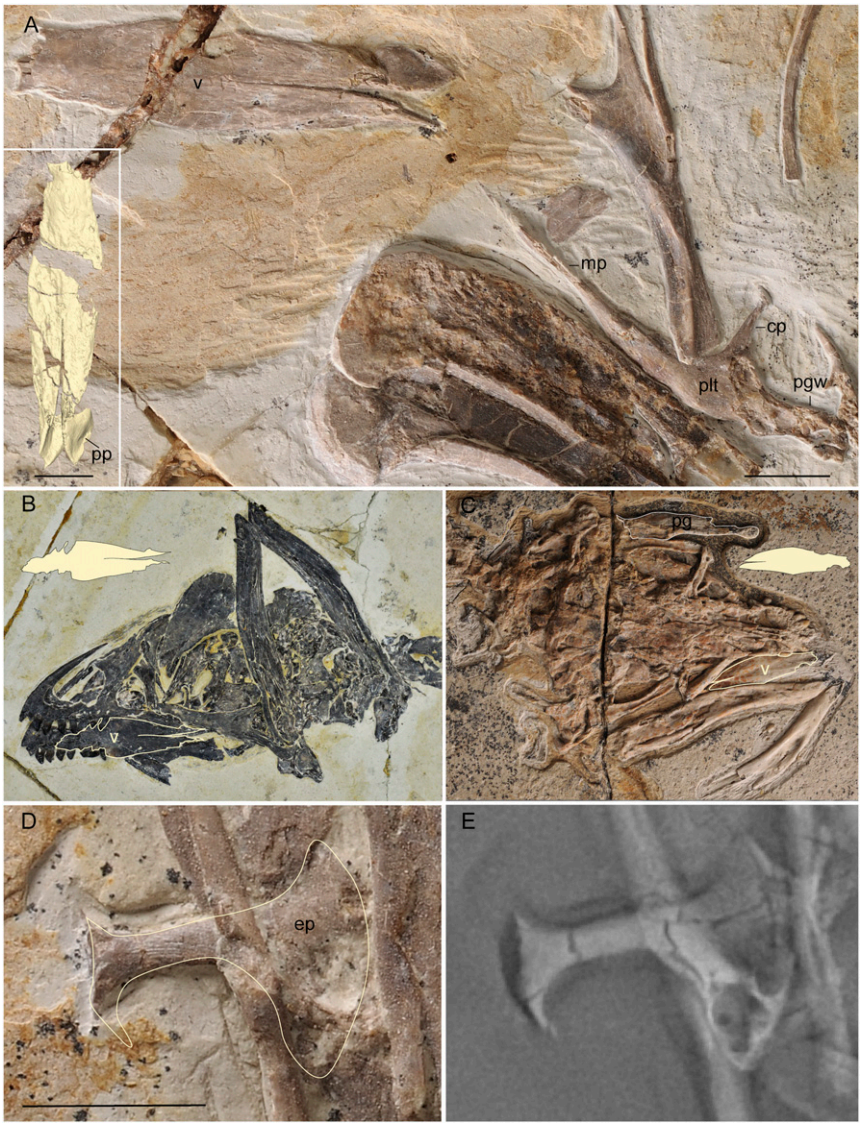

Fig. 3. Comparisons of identifiable vomers (in yellow) in IVPP V19058 and previously published specimens of *Sapeornis*. (*A*) Detailed photograph and ventral 3D model snapshot of the vomer, IVPP V19058. (*B*) Photograph of the skull, STM 16–18. (*C*) Photograph of the skull, IVPP V13275. (*D*) Detailed photograph of the ectopterygoid, IVPP V19058. (*E*) CL slice of IVPP V19058. Abbreviations: cp, choanal process; ep, ectopterygoid; mp, maxillary process of palatine; pg, pterygoid; pgw, pterygoid wing of palatine; plt, palatine; pp, caudodorsal process of vomer; and v, vomer. (Scale bar: 5 mm.)

(38). The element identified in these 2 specimens displays the same fused cranial portion with diverging caudal flanges and convex lateral margins, confirming our identification of the disarticulated vomer in IVPP V19058 (Fig. 3).

The vomer in IVPP V19058 was extracted from the slab, scanned using high-resolution computed tomography (CT), and reconstructed as a 3D model (Fig. 3*A* and interactive 3D model available in Figshare). In 3D, the complete morphology of the vomer in *Sapeornis* is more complex. The fused cranial portion is dorsoventrally thin and plate-like, whereas the caudal flanges each have a triangular leaflike process on the dorsal surface which is not visible in 2D. This feature, here referred to as the caudodorsal process, is somewhat deformed by compression in IVPP V19058 (Fig. 3*A*). Although both of the left and right caudodorsal processes are preserved inclined to the right, the left process is distorted similar to the right. Using references from nonavian dinosaurs and extant birds, we 3D retrodeformed the caudodorsal process to be oriented nearly 90° to the horizontal body of the vomer (Fig. 2*D*). Craniodorsally, a deep notch separates the caudodorsal process and the main body of the vomer, so the cranial margin of this process is strongly concave. The craniodorsal portion of this process is tapered (Fig. 2*D*).

In order to capture morphological changes across the dinosaur–bird transition, we also generated a 3D reconstruction of the vomer from the holotype of the early-diverging troodontid *Sinovenator changii* (IVPP V12615, Fig. 2*E*). The vomer morphology of *Sapeornis* is largely consistent with that of *Sinovenator* (whose morphology is considered typical of troodontids and other nonavian dinosaurs) (37, 39) in that the cranial portion is dorsoventrally flat and a similar caudodorsal process is present. The dorsoventrally flat and mediolaterally wide cranial portion of the vomer in extant paleognaths forms an extensive dorsoventrally overlapping contact surface with the maxillae, whereas in neognaths the cranial portion is less dorsoventrally flat, so that the lateral margins of the vomer form an articular surface with the maxilla. The flat morphology in *Sapeornis* indicates the presence of a paleognathous-like overlapping articulation with the maxillae. Although the cranial portion of the vomer is more

slender in *Sinovenator*, it is still dorsoventrally flat, indicating that it also had an overlapping contact with the maxillae as in other nonavian dinosaurs. In *Sinovenator*, the caudodorsal process is much more extensive than in *Sapeornis*, present along the entirety of the caudal flange (limited to the caudal half in *Sapeornis*) with the tapered cranial end forming a long, slender, rostrally directed process that extends dorsally over the fused cranial portion (Fig. 2*E*). The medial surface of the caudodorsal process is concave in both *Sapeornis* and *Sinovenator* (Fig. 3*A*), accommodating the pterygoids (37, 40).

A fan-shaped element with a slender process is identified as the ectopterygoid based on scans generated using X-ray microcomputed laminography (CL) (Fig. 3 *D* and *E*). The *Sapeornis* ectopterygoid is morphologically similar to that of *Archaeopteryx* and nonavian dinosaurs. It is unreduced with the jugal process distally expanded to form a firm contact with the jugal, whereas this element is absent in neornithines, releasing the pterygoid from the cranium and in turn allowing movement between the palate and the cranium. We further identify a slender bone, preserved between the right jugal and humerus, as the palatine, another element rarely preserved in Mesozoic birds (Fig. 3*A*). Although a jugal process is not preserved, a nonavian dinosaur like tetraradiate palatine cannot be ruled out since comparison with *Archaeopteryx* indicates that the delicate jugal process is easily broken off and lost during preservation (24, 25). A robust and strut-like structure preserved in *Sapeornis* IVPP V13275 is probably the pterygoid (Fig. 3*C*). Using information combined from these specimens we generate a preliminary reconstruction of the palate of *Sapeornis* (Fig. 2*C*). In the reconstruction, the ectopterygoid contacts the jugal as indicated by the well-developed jugal process, forming a rigid palate very similar to that of *Archaeopteryx* and deinonychosaurs (24–26), and the vomer embraces the pterygoids (and/or the parasphenoid rostrum) along the concave medial surface of the caudodorsal process. However, since the caudal portion of vomer contacts both the pterygoids and the parasphenoid rostrum in the Paleognathae and only the parasphenoid rostrum in the Neognathae, we cannot determine with the current evidence if the caudodorsal process embraces the parasphenoid rostrum in *Sapeornis*, whereas this contact is absent in nonavian theropods. The orientation of the isolated palatine is also difficult to determine precisely at this time. We tentatively identify the tapered end as cranial, based on comparison with neornithines.

Geometric Morphometric Analysis. In order to uncover the evolutionary processes of the palate and cranial kinesis from nonavian dinosaurs to modern birds, we conducted a comprehensive morphological study of palatal elements with an emphasis on the vomer. The dataset incorporates representatives from all 40 extant orders of the Neornithes as well as the extinct order Dinornithiformes, sampling 149 families and 183 genera (*SI Appendix*, Table S3). Despite the fact that the vomer is strongly reduced in several Neognathous clades, e.g., the Strisores, Columbaves, and Coraciimorphae (11, 17, 21), our approach demonstrates that it is still possible to quantify the pattern of shape variation of this element in the remaining crown birds, including the Anseriformes, Gruiformes, Aequorlitornithes, early-diverged members of Inopinaves, and Australaves with the exception of the Psittaciformes (Fig. 4). Our results also indicate that vomer morphology is highly consistent within orders and even in higher level clades, such that the vomer alone can be used to differentiate between major groups of neognaths (Fig. 4).

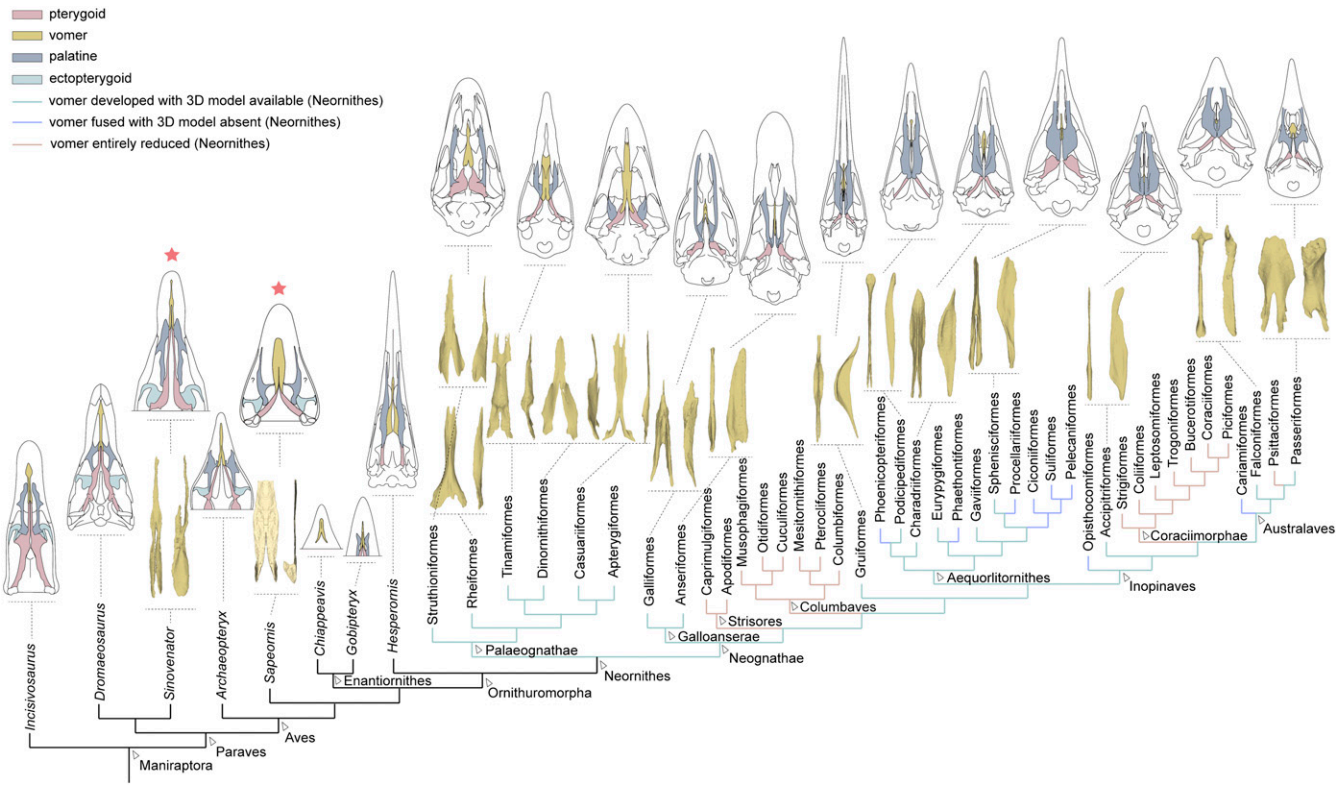

Fig. 4. Palatal evolution from nonavian dinosaurs to crown birds. Cladogram was simplified and modified from previous publications (2, 19, 35, 41–43). Palate of *Incisivosaurus*, *Dromaeosaurus*, and *Sinovenator* was reconstructed and modified from previous publications (35–37, 41, 44, 45) and the vomer extracted in this study; palate of *Archaeopteryx*, *Chiappeavis*, *Gobipteryx*, *Hespeornis*, and *Tinamous* was modified from previous publications (25, 27, 46–48). Red stars indicate the key taxa in this study. Data from refs. 2, 19, 25, 27, 35–37, and 41–48.

Based on these results, we reconstructed 3D models of the vomer for 17 representatives of the 24 orders of neornithines in which the vomer remains (*SI Appendix*, Table S3). Using these models together with the data from *Sapeornis* and *Sinovenator*, we conducted a 3D geometric morphometric (GMM) analysis of the vomer with a generalized Procrustes analysis (GPA) and a principal component analysis (PCA) (for landmark locations, see *SI Appendix*, Fig. S1). The PCA results place *Sapeornis* and *Sinovenator* close to each other and clustered with the Paleognathae, which is distinctly separated from the Neognathae. A Procrustes ANOVA and a likelihood-based phylogenetic generalized least squares (PGLS) analysis were then conducted on the data to quantitatively test this divergence, returning values indicating significant differences ($F_{1,37} = 7.232$, P value < 0.001; Wilks $\lambda = 0.039$, P value < 0.009, respectively) between the Paleognathae and the Neognathae (*SI Appendix*, Table S2). Phylogenetic signal analyses using the K_{mult} statistic also revealed the presence of a significant degree of a phylogenetic signal in the shape variables ($K_{mult} = 0.5546$, P value < 0.002). These results indicate that vomer morphology has a relatively strong phylogenetic signal, confirming that it can be used to identify high-order avian groups (Fig. 5 and *SI Appendix*).

Visualization of the PCA results from the GMM analysis indicate that variation in PC1 captures the relative length of the fused cranial portion of the vomer, equivalent to the position where the main body diverges caudally. In this axis and PC3, the Paleognathae and Neognathae largely overlap each other (Fig. 5 *A* and *B* and *SI Appendix*, Fig. S2 *A* and *B*). In PC2, lower scores indicate that the cranial fused portion of the vomer body is dorsoventrally thin and horizontally extensive, and the caudal flange is proportionately longer and more caudolaterally expanded (3D visualizations of the shape variation along PC1, -2, and -3 available in Figshare). The Paleognathae (consensus to negative values) and Neognathae (consensus to positive values) overall separate from each other along this axis with minimal overlap (Fig. 5 *A* and *C*). In the Paleognathae, *Dromaius* falls within the lower portion of the positive morphospace along PC2, which may be explained by the fact that its fused cranial portion is relatively long so that the caudal flange is proportionately shorter than in other paleognaths. However, it maintains the large overlapping articulation with the maxilla typical of the paleognathous vomer morphology visible in both 2D and 3D observations (Fig. 4 and *SI Appendix*, Fig. S3*A*). In the Neognathae, the relatively negative position of representatives of the Aequorlitornithes, including the Charadriiformes, Podicipediformes, and Gruiformes, is likely due to the mediolaterally expanded sheet present on the dorsal surface of the cranial portion of the vomer in these groups, in which a ridge is present, extending dorsoventrally (*SI Appendix*, Fig. S4). Since the maxilla laterally contacts this ridge, rather than having an overlapping articulation with the mediolaterally expanded sheet-like portion, this morphology still falls within the typical neognathous condition. Based on the dominating negative position of the Paleognathae and the positive position of the Neognathae along PC2, the biggest differences between these 2 groups can be summarized as: 1) the presence of either a mediolateral (neognaths) or dorsoventral (paleognaths) articulation between the cranial portion of the vomer and the maxilla, and 2) differences in the range of contact with the parasphenoid rostrum (and the pterygoids in paleognaths), small in neognaths and extensive in paleognaths.

Discussion

Morphological and Kinetic Divergence of Paleognathae and Neognathae. The fundamental dichotomy at the base of Neornithes, the Paleognathae and the Neognathae, has previous been diagnosed largely based on the morphology of the palatine and pterygoid. The morphological variation and repeated reduction of the vomer in the Neognathae hindered comparison of this element between

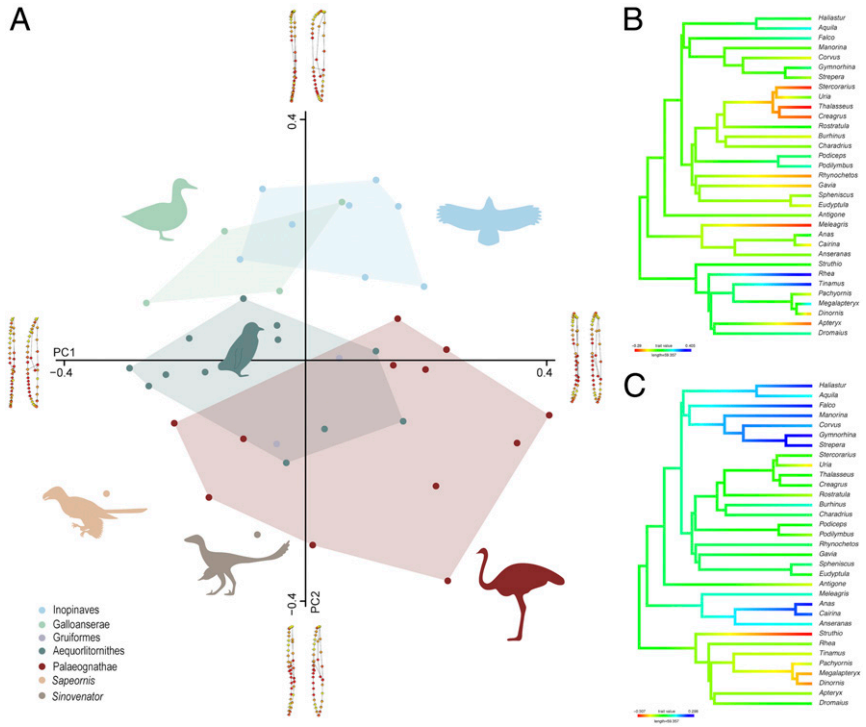

Fig. 5. (*A*) PCA result of vomer shape (PC1 and PC2). The red convex hull indicates the Paleognathae and the other colored convex hulls indicate major groups within the Neognathae; the warmer colored balls in the visualized vomer illustration indicate a stronger deformation area from the mean shape and vice versa. (*B*) Mapping of PC1 scores in Neornithes. (*C*) Mapping of PC2 scores in Neornithes, the warmer colored clades indicate a lower score and vice versa.

these 2 clades (7, 9, 17). However, the results of our quantitative study have made it possible to identify a morphological pattern of vomer in the Neognathae to allow comparison with the Paleognathae, and indicate that it is especially useful for distinguishing these 2 clades. Contact between the broad vomer and the parasphenoid rostrum, which provides structural support for the ventral surface of the cranium, was previously considered to be an apomorphy of the Paleognathae (17, 49, 50), whereas the neognath vomer was considered to have nearly entirely lost contact with the maxillae and the parasphenoid rostrum (16, 17). However, the results of our study indicate that all neognathous clades with a vomer maintain contacts with the parasphenoid rostrum and the maxillae, although the former is reduced and the latter differs from that of paleognaths. These differences are clearly expressed in the PCA results as negative and positive divergence along PC2 separating the Paleognathae and Neognathae. Visualization of the shape variation along PC2 (Fig. 5) shows that the Paleognathae possess a vomer that is overall more dorsoventrally flattened cranially, forming an extensive dorsoventral articulation with the maxillae, with a larger caudal flange, forming a larger surface for articulation with the parasphenoid. In contrast, the Neognathae possess a vomer that overall is narrower, presenting a more laterally oriented articulation with the maxilla and much less contact with the parasphenoid. Thus, the distinction between the Paleognathae and Neognathae is not the existence (or absence) of the vomer–parasphenoid rostrum contact, but rather the size and extent of this contact and the orientation of the vomer–maxillae articulation.

Further differences between the Paleognathae and Neognathae can be observed in the basipterygoid process of the parasphenoid and the contact between the vomer and pterygoids. The basipterygoid process is well developed in all of the paleognaths as in nonavian theropods (51), but absent in the neognaths except for the Galloanserae. However, the significantly rostral positions of this process in the Galloanserae indicate that this feature is not homologous with that of the Paleognathae (17).

Although a unique central or paleognathous rhynchokinesis was suggested for paleognaths (9, 12, 20), it was subsequently demonstrated that the "rhynchokinesis" in paleognaths is very limited and lacks a distinct bending zone during biting, which is present in neognaths. It was concluded that the bending of the upper bill in the Paleognathae was more likely an incidental consequence of the slender lateral and dorsal cranial elements during feeding, than a true form of cranial kinesis (11, 13, 14, 52). The dorsoventrally overlapping articulation with the maxillae and large embracing contact with the parasphenoid rostrum and pterygoids of the vomer, together with the pterygoid–cranium contact through the unreduced basipterygoid process in paleognaths all work together to prevent sliding movement between the palate–rostrum and the palate–cranium (*SI Appendix*, Fig. S3), and thus supports reinterpretations regarding cranial kinesis in this clade. Compared to the rigid paleognathous palate, the palate of neognaths is a delicate structure that provides a trade-off between stability and flexibility. The mediolateral articulation between the maxilla and vomer allows the rostrum to slide cranially along this contact, and the reduced contact with the parasphenoid allows decoupling of the palate and the cranium. These modifications of the vomer in shape and size considerably improved the flexibility of the neognathous skull relative to the plesiomorphic condition retained by paleognaths. The complete reduction of the vomer in some neognathous clades further increases palate mobility (Fig. 4).

Inferring Cranial Kinesis in Extinct Nonneornithine Paraves. Our morphological observations demonstrate similarity between the palatal elements in *Sapeornis*, *Sinovenator*, and the Paleognathae. This similarity of vomer is also quantitatively supported by the results of our GMM analysis: the close position of *Sapeornis* and *Sinovenator* to the Paleognathae in the PCA morphospace confirms the hypothesis that the morphology of the paleognathous palate is primitive (53), consistent with its primitive pattern of development (18). The similar vomer morphology in *Sapeornis*, *Sinovenator*, and paleognaths strongly suggests that these extinct taxa are similarly characterized by the low degree of flexibility observed in paleognaths and supports inferences that early bird crania had very limited, if any, kinetic ability (54, 55).

Identification of the ectopterygoid bone preserved in *Sapeornis* IVPP V10958 also supports the inferences based on vomer morphology regarding limited kinesis in this stem-avian lineage. The ectopterygoid has only been previously documented among birds in *Archaeopteryx* (24). The loss of this element is regarded as one of the major modifications evolved during the evolution of the modern avian skull from the dinosaurian condition. In nonavian dinosaurs this element is well developed, having an extensive large contact with the medial surface of the jugal and the lateral surface of the pterygoid. Reduction of the ectopterygoid and loss of its contact with the jugal decoupled the palate from the cranium, further facilitating the evolution of cranial kinesis in more derived birds. The ectopterygoid in *Sapeornis* IVPP V19058 resembles the morphology in *Archaeopteryx* and nonavian dinosaurs (Fig. 4). The jugal process is distally expanded where it contacts the jugal, indicating a rigid cranium–palatal complex. Limited cranial kinesis in *Archaeopteryx*, *Sapeornis*, and other stem-avians is further supported by additional cranial features such as the complete postorbital bar formed by the large, triangular postorbital (absent in most neornithines) (26), and the tight articulations between the robust jugal and the quadratojugal caudally and the maxilla cranially, all features also observed in the akinetic skull of nonavian dinosaurs (22). In comparison, the postorbital bar is absent and the thin rod-like jugal in neornithines is fused to the quadratojugal, allowing greater flexion (56).

Very little palatal data are available for the Enantiornithes, the dominant clade of Cretaceous terrestrial birds. The best data come from the Late Cretaceous *Gobipteryx* (28, 29), and an element was ambiguously identified as the vomer in Early Cretaceous *Chiappeavis* (27). Despite the poor preservation, the overall mediolaterally extensive morphology of the vomer in *Chiappeavis* suggests a condition similar to that in *Sapeornis* and paleognaths. The condition in *Gobipteryx* is more complex. The presence of well-developed basipterygoid processes indicate the pterygoid–cranium contact is retained. The vomer is caudally forked with broadly expanded dorsal flanges, reminiscent of the condition in nonavian theropods, *Sapeornis,* and paleognaths. However, the fused cranial portion contacts the cranial portion of the maxillae laterally similar to the neognathous condition (29). Since enantiornithines and ornithuromorphs diverged for more than 130 Ma, we infer that the unique palatal architecture in Late Cretaceous taxa like *Gobipteryx* arose independent of the crown birds and cannot be treated as the ancestral state for living birds. The current evidence suggests cranial kinesis would have been limited in *Gobipteryx*, although more specimens preserving key morphologies i.e., the vomer–palatine–pterygoid system are necessary to better understand the evolution of palate and cranial kinesis in this lineage.

Among nonneornithine ornithurines, *Hesperornis* from the Late Cretaceous has been previously suggested to be prokinetic (57). However, the palatine and vomer are very poorly preserved in this taxon (31, 32), and thus there is no unequivocal anatomical information capable of supporting this interpretation. In *Ichthyornis*, another Late Cretaceous ornithurine, the mobile joint between the jugal bar and quadrate and the narrow morphology of the palatine may indicate the presence of some cranial kinesis (30). However, the absence of a nasofrontal hinge and the presence of a well-developed maxillary shelf (which may have contacted the vomer dorsoventrally similar to the condition in paleognaths) indicate that without further data, we cannot exclude the possibility that cranial kinesis was poorly developed or that a unique kinetic system was independently evolved in this lineage, as is possible in *Gobipteryx*.

Origins of Cranial Kinesis. Multiple lines of the evidence indicate that the Paleognathae retain the plesiomorphic morphology of the palate inherited from nonavian dinosaurs and as a result, can be used to infer limited cranial kinesis in stem birds and nonavian dinosaurs. The palatal morphology of stem paleognaths such as the Paleogene *Lithornis* and *Paleotis* is very similar to that of extant paleognathous taxa (58, 59), indicating that the primitive palatal morphology in extant paleognaths is not likely to be a reversal. In contrast to the paleognathous palate, the neognathous palate is much more modified. Our study indicates that modification of the vomer played a prominent role in this evolutionary transition. With the pterygoids remarkably shortened in both neornithine clades relative to nonavian dinosaurs, the paleognaths and neognaths maintained the palatal stability and function through different mechanisms: the Paleognathae retained and enhanced the plesiomorphically broad vomer, which obstructs the kinesis; in contrast, the vomer was reduced and the palatines became significantly enlarged in the Neognathae, allowing sliding movements within the palatal complex and thus providing the potential for cranial kinesis. Based on this analysis, we preliminarily suggest that the remarkable flexibility of the modern avian skull is an innovation of the Neognathae that evolved after its divergence from the Paleognathae in the Late Cretaceous. Cranial kinesis in extant birds allows numerous advantages, such as increased gape for swallowing large prey, more rapid opening and closing of the bill, increased bite force, greater precision in food selection, and specialized feeding strategies such as mud probing and filtering (9–11). All of these functions serve to improve feeding performance and therefore can be considered evolutionarily advantageous.

According to both molecular and fossil evidence, the divergence between the Paleognathae and the Neognathae occurred during the Late Cretaceous (2, 4, 5). After the Cretaceous-Paleogene (K-Pg) mass extinction, the Neognathae experienced a rapid radiation, ultimately resulting in the modern diversity of over 10,000 species. Conversely, the Paleognathae only comprises 60 species with extremely low interspecific morphological diversity compared to the Neognathae (1, 2, 11, 19). The extinction of pterosaurs, nonavian dinosaurs, enantiornithines, and early-diverging ornithuromorph lineages at the end of the Cretaceous would have left numerous ecological niches vacant, providing opportunities for diversification during the early Paleogene. At the same time, cooling of the climate would have isolated populations, also increasing the likelihood of speciation events (5, 6). Despite similar opportunities for diversification, the Paleognathae and the Neognathae experienced very different evolutionary rates, culminating in huge differences in both taxonomic and morphological diversity. The greater efficiency and evolutionary plasticity of the neognathous feeding mechanism afforded by the evolution of cranial kinesis may have increased the adaptability of this clade, allowing them to diversify into a wider array of ecological niches compared to the paleognaths, and thus ultimately be at least partially responsible for the current success of the neognathous radiation.

Methods

CT Scans and Digital Reconstructions. CT scans of the vomer of *Sapeornis* IVPP V19058 and the skull of *Sinovenator* IVPP V12615 were generated with the 225-kV micro-CT, and CL scanning of the skull of *Sapeornis* IVPP V19058 was generated using X-ray microcomputed laminography at the Key Laboratory of Vertebrate Evolution and Human Origin, IVPP, Chinese Academy of Sciences, Beijing, China. Scanning of the skulls of modern birds from Natural History Museum of University of New England and Queensland Museum in the checking list were generated with the Phoenix v-tome-x Industrial High-Resolution CT at the University of New England. The 3D reconstructions and the fixing of 3D models were created and completed with the software Mimics and 3-matic (version 16.1). The broken cranial and caudal portions in the *Sapeornis* model were joined, based on observation of the actual specimen, which shows that this separation is from the breakage of the whole slab, rather than absence of the bone between them. The more complete left half of the model was then mirrored to fill missing data in the right half. The distorted caudodorsal process was warped to the vertical plane symmetrically, using the models of *Sinovenator* and *Struthio* as references.

GMM Analysis. On each vomer, 5 anatomical landmarks were digitized, and 43 semilandmarks were placed equidistantly along the curves of the bone (for landmark definitions, see *SI Appendix, Supplementary Methods* and for landmark locations, see *SI Appendix*, Fig. S1) to capture its shape in 3 dimensions using Checkpoint software. Once all of the landmarks were digitized, they were imported into R version 3.4.4 for further analyses. We performed GPA (60, 61) on all landmarks, implemented in the ProcSym() function from the R package "Morpho" (62), to rotate, translate, and scale landmark configurations to unit centroid size (CS, square root of squared differences between landmark coordinates and centroid coordinates) (63). To visualize the multivariate ordination of the aligned Procrustes coordinates, a PCA was performed afterward. The significance of the observed shape changes between the Paleognathae and the Neognathae was evaluated by performing a Procrustes ANOVA on aligned Procrustes coordinates using the function procD.lm() from the R package "geomorph" (61, 64). Shape changes have been visualized using the function plotRefToTarget.heat() from the "landmark-test" (available at https://github.com/TGuillerme/landmark-test), which allows the addition of heat maps to better visualize the landmarks variation. This function is a modified version of the function plotRefToTarget() from the "geomorph" R package.

Phylogeny and Comparative Methods. To generate a phylogenetic tree containing all taxa of the Neornithes included in this study, we generated a composite time-calibrated topology. Using the function maxCladeCred() from the R package "phangorn" (65), a maximum clade credibility tree of the living species in the analysis was constructed from a set of 100 molecular trees (http://birdtree.org) (1) with the following modifications: 1) replacement of the Paleognathae with the time-calibrated tree including the extinct Dinornithiformes (43); and 2) *Antigone rubicunda* was treated as the sister group of all of the other non-Gallosanserae neognaths (2). Phylogenetic signal was calculated for the shape data using the K_{mult} statistic, a method that measures the similarity of trait values in relation to a Brownian motion model of evolution. It is specifically designed for the challenges of working with high-dimensional landmark configurations (66). We used a novel likelihood-based multivariate PGLS linear model to account for the nonindependence among observations due to shared phylogenetic history (67, 68). The PGLS is implemented in the R package "mvMORPH" and performed using the function mvgls(); significance of the model has been tested using the function manova.gls() by means of Wilks' lambda (69). In order to visualize the distribution of the shape variables on the phylogenetic tree, the first 3 PC scores were mapped on the phylogeny using the contMap() function from the R package "phytools" (70).

Data Availability. The 3D vomer models, landmark data, and phylogenetic tree are publicly available on Figshare (DOI: 10.6084/m9.figshare.7769279.v2). IVPP V19058 is housed at the Institute of Vertebrate Paleontology and Paleoanthropology in Beijing, China.

ACKNOWLEDGMENTS. We acknowledge D. Li for specimen preparation; W. Gao for photography; H. Janetzki from the Queensland Museum and L. Tsang from the Australian Museum for help with organizing the extant specimens; and L. Dong, J. Lu, R. Flavel, and M. White for help with CT scanning and 3D reconstructions. This research was supported by a Postdoctoral Research Fellowship from the University of New England (H.H.); the State Key Laboratory of Paleobiology and Stratigraphy, the Nanjing Institute of Geology and Paleontology, Chinese Academy of Sciences grant 183110 (H.H.); and the National Natural Science Foundation of China grant 41688103 (Z.Z.).

1. W. Jetz, G.-H. Thomas, J.-B. Joy, K. Hartmann, A.-O. Mooers, The global diversity of birds in space and time. *Nature* **491**, 444–448 (2012).
2. R.-O. Prum *et al.*, A comprehensive phylogeny of birds (Aves) using targeted next-generation DNA sequencing. *Nature* **526**, 569–573 (2015).
3. J.-K. O'Connor, The trophic habits of early birds. *Palaeogeogr. Palaeoclimatol. Palaeoecol.* **513**, 178–195 (2019).
4. J.-A. Clarke, C.-P. Tambussi, J.-I. Noriega, G.-M. Erickson, R.-A. Ketcham, Definitive fossil evidence for the extant avian radiation in the Cretaceous. *Nature* **433**, 305–308 (2005).
5. S. Claramunt, J. Cracraft, A new time tree reveals Earth history's imprint on the evolution of modern birds. *Sci. Adv.* **1**, e1501005 (2015).
6. S.-L. Brusatte, J.-K. O'Connor, E.-D. Jarvis, The origin and diversification of birds. *Curr. Biol.* **25**, R888–R898 (2015).

7. R.-G. Bout, G.-A. Zweers, The role of cranial kinesis in birds. *Comp. Biochem. Physiol. A Mol. Integr. Physiol.* **131**, 197–205 (2001).
8. B. A. Bhullar *et al*., How to make a bird skull: Major transitions in the evolution of the avian cranium, paedomorphosis, and the beak as a surrogate hand. *Integr. Comp. Biol.* **56**, 389–403 (2016).
9. R.-L. Zusi, A functional and evolutionary analysis of rhynchokinesis in birds. *Smithson. Contrib. Zool.* **395**, 1–40 (1984).
10. S.-M. Estrella, J.-A. Masero, The use of distal rhynchokinesis by birds feeding in water. *J. Exp. Biol.* **210**, 3757–3762 (2007).
11. S. W. S. Gussekloo *et al*., Functional and evolutionary consequences of cranial fenestration in birds. *Evolution* **71**, 1327–1338 (2017).
12. W.-J. Bock, Kinetics of the avian skull. *J. Morphol.* **11**, 1–42 (1964).
13. S. W. S. Gussekloo, R.-G. Bout, Cranial kinesis in palaeognathous birds. *J. Exp. Biol.* **208**, 3409–3419 (2005).
14. S. W. S. Gussekloo, R.-G. Bout, The kinematics of feeding and drinking in palaeognathous birds in relation to cranial morphology. *J. Exp. Biol.* **208**, 3395–3407 (2005).
15. M.-M. Dawson, K.-A. Metzger, D.-B. Baier, E.-L. Brainerd, Kinematics of the quadrate bone during feeding in mallard ducks. *J. Exp. Biol.* **214**, 2036–2046 (2011).
16. E.-N. Kurochkin, Morphological differentiation of the palaeognathous and neognathous birds. *Cour. Forschungsinst. Senckenb.* **181**, 79–88 (1995).
17. R.-L. Zusi, B.-C. Livezey, Variation in the os palatinum and its structural relation to the palatum osseum of birds (Aves). *Ann. Carnegie Mus.* **75**, 137–180 (2006).
18. E.-E. Maxwell, Comparative ossification and development of the skull in palaeognathous birds (Aves: Palaeognathae). *Zool. J. Linn. Soc.* **156**, 184–200 (2009).
19. F. Gill, D. Donsker, IOC World Bird List, version 8.2, 10.14344/IOC.ML.8.2 (2018).
20. A.-M. Simonetta, On the mechanical implications of the avian skull and their bearing on the evolution and classification of birds. *Q. Rev. Biol.* **35**, 206–220 (1960).
21. M.-T. Jollie, Comments on the phylogeny and skull of the asseriformes. *Auk* **75**, 26–35 (1958).
22. C.-M. Holliday, L.-M. Witmer, Cranial kinesis in dinosaurs: Intracranial joints, protractor muscles, and their significance for cranial evolution and function in diapsids. *J. Vertebr. Paleontol.* **28**, 1073–1088 (2008).
23. Z.-H. Zhou, The Jehol Biota, an Early Cretaceous terrestrial Lagerstätte: New discoveries and implications. *Natl. Sci. Rev.* **1**, 543–559 (2014).
24. A. Elzanowski, P. Wellnhofer, Cranial morphology of *Archaeopteryx*: Evidence from the seventh skeleton. *J. Vertebr. Paleontol.* **16**, 81–94 (1996).
25. G. Mayr, B. Pohl, S. Hartman, D.-S. Peters, The tenth skeletal specimen of *Archaeopteryx*. *Zool. J. Linn. Soc.* **149**, 97–116 (2007).
26. O. W. M. Rauhut, C. Foth, H. Tischlinger, The oldest *Archaeopteryx* (Theropoda: Avialiae): A new specimen from the Kimmeridgian/Tithonian boundary of Schamhaupten, Bavaria. *PeerJ* **6**, e4191 (2018).
27. J.-K. O'Connor, X.-T. Zheng, H. Hu, X.-L. Wang, Z.-H. Zhou, The morphology of *Chiappeavis magnapremaxillo* (Pengornithidae: Enantiornithes) and a comparison of aerodynamic function in Early Cretaceous avian tail fans. *Vertebr. Palasiat.* **55**, 41–58 (2017).
28. A. Elzanowski, Skulls of *Gobipteryx* (Aves) from the upper Cretaceous of Mongolia. *Acta Palaeontol. Pol.* **37**, 153–165 (1977).
29. L.-M. Chiappe, M. Norell, J. Clark, A new skull of *Gobipteryx minuta* (Aves: Enantiornithes) from the Cretaceous of the Gobi Desert. *Am. Mus. Novit.* **3346**, 1–15 (2001).
30. D.-J. Field *et al*., Complete *Ichthyornis* skull illuminates mosaic assembly of the avian head. *Nature* **557**, 96–100 (2018).
31. P.-D. Gingerich, Skull of *Hesperornis* and early evolution of birds. *Nature* **243**, 70 (1973).
32. A. Elzanowski, New observations on the skull of *Hesperornis* with reconstructions of the bony palate and otic region. *Postilla* **207**, 1–20 (1991).
33. J.-K. O'Connor, L.-M. Chiappe, A revision of enantiornithine (Aves: Ornithothoraces) skull morphology. *J. Syst. Palaeontology* **9**, 135–157 (2011).
34. Z. Zhou, F. Zhang, Largest bird from the Early Cretaceous and its implications for the earliest avian ecological diversification. *Naturwissenschaften* **89**, 34–38 (2002).
35. X. Xu, M.-A. Norell, X. L. Wang, P.-J. Makovicky, X. C. Wu, A basal troodontid from the Early Cretaceous of China. *Nature* **415**, 780–784 (2002).
36. Y. L. Yin, R. Pei, C. F. Zhou, Cranial morphology of *Sinovenator changii* (Theropoda: Troodontidae) on the new material from the Yixian Formation of western Liaoning, China. *PeerJ* **6**, e4977 (2018).
37. T. Tsuihiji *et al*., An exquisitely preserved troodontid theropod with new information on the palatal structure from the Upper Cretaceous of Mongolia. *Naturwissenschaften* **101**, 131–142 (2014).
38. Y. Wang *et al*., A previously undescribed specimen reveals new information on the dentition of *Sapeornis chaoyangensis*. *Cretac. Res.* **74**, 1–10 (2017).
39. M.-A. Norell *et al*., A review of the Mongolian Cretaceous dinosaur *Saurornithoides* (Troodontidae: Theropoda). *Am. Mus. Novit.* **3654**, 1–63 (2009).
40. J.-M. Clark, M.-A. Norell, T. Rowe, Cranial anatomy of *Citipati osmolskae* (Theropoda, Oviraptorosauria), and a reinterpretation of the holotype of *Oviraptor philoceratops*. *Am. Mus. Novit.* **3364**, 1–24 (2002).
41. X. Xu, Y.-N. Cheng, X.-L. Wang, C.-H. Chang, An unusual oviraptorosaurian dinosaur from China. *Nature* **419**, 291–293 (2002).
42. H. Hu, J.-K. O'Connor, First species of Enantiornithes from Sihedang elucidates skeletal development in Early Cretaceous enantiornithines. *J. Syst. Palaeontology* **15**, 909–926 (2017).
43. T. Yonezawa *et al*., Phylogenomics and morphology of extinct paleognaths reveal the origin and evolution of the ratites. *Curr. Biol.* **27**, 68–77 (2017).
44. A.-M. Balanoff, X. Xu, Y. Kobayashi, Y. Matsufune, M.-A. Norell, Cranial osteology of the theropod dinosaur *Incisivosaurus gauthieri* (Theropoda: Oviraptorosauria). *Am. Mus. Novit.* **3651**, 1–35 (2009).
45. L.-M. Witmer, The evolution of the antorbital cavity of archosaurs: A study in soft-tissue reconstruction in the fossil record with an analysis of the function of pneumaticity. *J. Vertebr. Paleontol.* **17**, 1–76 (1997).
46. A. Elzanowski, Cretaceous birds and avian phylogeny. *Cour. Forschungsinst. Senckenb.* **181**, 37–53 (1995).
47. G. Heilman, *Origin of Birds* (Witherby, London, 1926), p. 209.
48. W.-K. Parker, VIII. On the structure and development of the skull in the ostrich tribe. *Philos. Trans. R. Soc. Lond.* **156**, 113–183 (1866).
49. J. Cracraft, Phylogeny and evolution of the ratite birds. *Ibis* **116**, 494–521 (1974).
50. P. Johnston, New morphological evidence supports congruent phylogenies and Gondwana vicariance for palaeognathous birds. *Zool. J. Linn. Soc.* **163**, 959–982 (2011).
51. T.-H. Frazzetta, K.-V. Kardong, Biomechanics (Communication arising): Prey attack by a large theropod dinosaur. *Nature* **416**, 387–388 (2002).
52. S. W. S. Gussekloo, G.-A. Zweers, The paleognathous pterygoid palatinum complex. A true character? *Neth. J. Zool.* **49**, 29–43 (1999).
53. S. W. S. Gussekloo, R.-G. Bout, Non-neotenous origin of the palaeognathous (Aves) pterygoid-palate complex. *Can. J. Zool.* **80**, 1491–1497 (2002).
54. O. W. M. Rauhut, New observations on the skull of *Archaeopteryx*. *PalZ* **88**, 211–222 (2014).
55. M. Wang, J.-K. O'Connor, Z.-H. Zhou, *A Taxonomical Revision of the Confuciusornithiformes (Aves: Pygostylia)* (Vertebr. Palasiat, 2018).
56. M. Wang, H. Hu, A comparative morphological study of the jugal and quadratojugal in early birds and their dinosaurian relatives. *Anat. Rec. (Hoboken)* **300**, 62–75 (2017).
57. P. Bühler, L.-D. Martin, L.-M. Witmer, Cranial kinesis in the Late Cretaceous birds *Hesperornis* and *Parahesperornis*. *Auk* **105**, 111–122 (1988).
58. L. Leonard, G.-J. Dyke, M. van Tuinen, A new specimen of the fossil palaeognath *Lithornis* from the Lower Eocene of Denmark. *Am. Mus. Novit.* **3491**, 1–11 (2005).
59. G. Mayr, The middle Eocene European "ratite" *Palaeotis* (Aves, Palaeognathae) restudied once more. *PalZ* **89**, 503–514 (2015).
60. F.-J. Rohlf, D. Slice, Extensions of the Procrustes method for the optimal superimposition of landmarks. *Syst. Biol.* **39**, 40–59 (1990).
61. C. Goodall, Procrustes methods in the statistical analysis of shape. *J. R. Stat. Soc.* **53**, 285–339 (1991).
62. S. Schlager, "Morpho and Rvcg: Shape analysis in R" in *Statistical Shape and Deformation Analysis*, G. Zheng, S. Li, G. Szekely, Eds. (Elsevier, 2017), pp. 217–256.
63. F.-L. Bookstein, *Morphometric Tools for Landmark Data* (Cambridge University Press, 1991).
64. D.-C. Adams, E. Otárola-Castillo, geomorph: An R package for the collection and analysis of geometric morphometric shape data. *Methods Ecol. Evol.* **4**, 393–399 (2013).
65. K.-P. Schliep, Phangorn: Phylogenetic analysis in R, version 2.5.5. *Bioinformatics* **27**, 592–593 (2011).
66. D.-C. Adams, A generalized K statistic for estimating phylogenetic signal from shape and other high-dimensional multivariate data. *Syst. Biol.* **63**, 685–697 (2014).
67. M.-L. Zelditch, D.-L. Swiderski, H.-D. Sheets, *Geometric Morphometrics for Biologists* (Academic Press, 2012).
68. D.-C. Adams, M.-L. Collyer, Permutation tests for phylogenetic comparative analyses of high-dimensional shape data: what you shuffle matters. *Evolution* **69**, 823–829 (2015).
69. J. Clavel, G. Escarguel, G. Merceron, mvMORPH: An R package for fitting multivariate evolutionary models to morphometric data. *Methods Ecol. Evol.* **6**, 1311–1319 (2015).
70. L.-J. Revell, phytools: An R package for phylogenetic comparative biology (and other things). *Methods Ecol. Evol.* **3**, 217–223 (2012).